Zoosyst. Evol. 102 (2) 2026, 687–699 | DOI 10.3897/zse.102.163746

PENSOFT

für Naturkunde MUSEUM FÜR NATURKUNDE BERLIN

Mitochondrial genomes resolve phylogenetic conflicts and lineage-specific adaptive dynamics in Ophiuroidea: insights from deep-sea lineages

Weihao Xu[1,2], Jieying Na[3], Kexin Gao[1], Xinyu Gu[1], Yadong Zhou[3], Ruiyan Zhang[3], Jin Sun[1], Dongsheng Zhang[3,4]

1 *Institute of Evolution & Marine Biodiversity, Ocean University of China, Qingdao, China*
2 *Haide College, Ocean University of China, Qingdao, China*
3 *State Key Laboratory of Submarine Geoscience, Second Institute of Oceanography, Ministry of Natural Resources, Hangzhou, China*
4 *State Key Laboratory of Submarine Geoscience, School of Oceanography, Shanghai Jiao Tong University, Shanghai 200030, China*

https://zoobank.org/2059C2F1-B8E0-4311-9372-BD37A449014C

Corresponding authors: Dongsheng Zhang (dszhang@sio.org.cn); Jin Sun (jin_sun@ouc.edu.cn)

Academic editor: Carsten Lüter ♦ **Received** 1 July 2025 ♦ **Accepted** 18 March 2026 ♦ **Published** 23 April 2026

Abstract

Ophiuroidea, the most diverse class of echinoderms, occupy habitats ranging from coastal zones to deep sea, offering unique insights into evolutionary adaptation and biogeography. Despite their ecological prominence, the phylogenetic relationships within Ophiuroidea still remain contentious, and their adaptive mechanisms to extreme environments such as the deep sea are poorly understood. Here, we present four newly sequenced mitochondrial genomes from deep-sea species (*Ophioctenella acies*, *Ophiura* cf. *irrorata*, *Ophiactis profundi*, and *Ophiocreas nudusoralis*) and integrate them with 52 published genomes to reconstruct the phylogeny, divergence history, and adaptive evolution. Using Maximum Likelihood and Bayesian Inference approaches, we resolved a robust phylogeny that supports the monophyly of major orders (Ophiurida, Euryalida, Amphilepidida, and Ophiacanthida) and clarifies previously unstable family-level relationships. Divergence time estimation and ancestral state reconstruction revealed that deep-sea lineages diversified primarily during the Jurassic and Cretaceous, with contrasting evolutionary trajectories: Ophiacanthida and Euryalida originated in deep sea and repeatedly colonized shallow waters, while Ophioleucida and Ophiurida expanded from shallow to deep environments. Surprisingly, mitochondrial gene rearrangement patterns and positive selection signals showed no significant correlation with pressures or habitats (e.g., depth, chemosynthesis), but instead varied markedly between lineages, with Ophintegrida exhibiting higher structural plasticity than the conserved Euryophiurida. By leveraging the most comprehensive mitochondrial dataset to date, our work provides insights into the phylogenetic history, biogeographic dispersal, and molecular evolution of Ophiuroidea, establishing a foundation for future studies on echinoderm diversification and adaptation.

Key Words

Biogeography, Chemosynthesis, deep sea, mitochondrial genome, Ophiuroidea

Introduction

The Ophiuroidea (also called brittle stars) is regarded as the most diverse group within the phylum Echinodermata, occupying a broad range of ecological niches that span from tropical to polar regions and from coastal waters to the deep sea (O'Hara et al. 2011; Stöhr et al. 2012). It plays diverse and vital roles in marine ecosystems, serving as suspension feeders, scavengers, and opportunistic feeders (Emson et al. 1991; Fratt and Dearborn 1984). The class Ophiuroidea diverged relatively recently compared to other classes in Echinodermata, approximately 260 million years ago (Ma) (O'Hara et al. 2014; O'Hara et al. 2017; Sun et al. 2023). These characteristics

Copyright *Xu, W. et al.* This is an open access article distributed under the terms of the Creative Commons Attribution License (CC BY 4.0), which permits unrestricted use, distribution, and reproduction in any medium, provided the original author and source are credited.

render it an exemplary material for the study of evolution (O'Hara et al. 2014). Mladenov and Emson (1988) analyzed the population density, body size structure, and reproductive adaptations of ophiuroids, exploring their evolutionary strategies in different habitats. Galaska et al. (2017) compared mitochondrial DNA (mtDNA) and single-nucleotide polymorphisms (SNPs) in ophiuroid species from different ecological environments, while O'Hara et al. (2014) investigated the phylogenetic relationships, divergence times, and adaptive evolution characteristics of the Ophiuroidea through genomic studies.

Phylogenetic analysis is fundamental to evolutionary research. Initial classification of Ophiuroidea by Matsumoto (1917) divided it into two subclasses, i.e. Oegophiurida and Phrynophiurida, later refined by Fell (1960). Smith et al. (1995) first applied combined morphological and molecular data to establish a phylogeny that long recognized two orders: Ophiurida and the Euryalida. O'Hara et al. (2014) reconstructed a phylogeny focusing on the ophiuroids based on amino acid sequences. Recent works classified Ophiuroidea into two major clades, Ophintegrida, which comprises four orders (Amphilepidida, Ophioleucida, Ophiacanthida and Ophioscolecida), and Euryophiurida, which comprises two orders (Ophiurida and Euryalida) (O'Hara et al. 2017; O'Hara et al. 2018). Nevertheless, uncertainties persist regarding the phylogenetic relationships within certain orders and lower taxonomic levels, particularly within the families Ophiactidae, Ophiopteridae, and Ophiopsilidae (O'Hara et al. 2017), as well as Ophiuridae (Sun et al. 2023). The mitochondrial genome has also been employed as an invaluable tool for identifying phylogenetic relationships of metazoans in previous researches (Chen et al. 2022; Li et al. 2021; Mikkelsen et al. 2018; Na et al. 2024; Sun et al. 2023), owing to its small size, maternal inheritance, infrequent recombination, and rapid evolutionary rate (Boore et al. 1998; Elson and Lightowlers 2006; Gissi et al. 2008; Lavrov and Lang 2005). To date, however, only 53 complete mitochondrial genomes from more than 2000 Ophiuroidea species were sequenced, and phylogenetic analysis of Ophiuroidea based on mitochondrial genomes are still limited (Chen et al. 2022; Galaska et al. 2019; Lee et al. 2019; Li et al. 2021; Na et al. 2024; Sun et al. 2023). The phylogenetic structure within the Ophiuroidea is notably inconsistent, a consequence of the heterogeneous mitochondrial genome datasets and phylogenetic analysis methods. With the growing accumulation of mitochondrial genome data, the phylogenetic relationships among brittle stars are becoming increasingly stable and reliable (Galaska et al. 2019; Lee et al. 2019; Na et al. 2024; Sun et al. 2023). However, the phylogenetic topologies reconstructed by Na et al. (2024) remain insufficiently stable, as the use of varying datasets and methods yielded nine distinct topologies out of the 18 trees generated.

Deep sea (> 200 m) is the largest and most untouched biome of the world, occupying about 66% of the bottom of the global ocean (Ramirez-Llodra et al. 2010), characterized by low temperatures, high hydrostatic pressure, food supply scarcity and constant darkness (Smith et al. 2008). To adapt to such a harsh environment, innovations on morphological, physiological and molecular traits have been developed in deep-sea species during the long evolutionary history (Campoy et al. 2023; Wang et al. 2019). Hydrothermal vents and cold seeps are chemosynthetic ecosystems, which were regarded as oases of the deep sea, supporting high organism abundance despite hostile environmental conditions like low oxygen levels, enriched hydrogen sulfide, methane and heavy metals. Macrofauna in these environments must adapt to high toxicity and anoxia, often acquiring chemosynthetic microbial symbionts (McMullin et al. 2000). Molecular evidences had been found in species inhabiting these reducing and non-reducing environments, such as *Archivesica* clams (Ip et al. 2021), *Bathymodiolus* mussels (Sun et al. 2017), siboglinid tubeworms (Li et al. 2019) and *Rimicaris* shrimps (Choi et al. 2025). Mitochondrial genome has been widely used for the study of extreme environment adaptation mechanisms, primarily manifested through genomic rearrangements and the emergence of selective pressures (da Fonseca et al. 2008; Garvin et al. 2015; Sun et al. 2019; Welch et al. 2014). Recent adaptation researches focused primarily on molluscs, annelids, ect. (Bebianno et al. 2018; Hui et al. 2018; Sun et al. 2017; Yang et al. 2019), while knowledge of the adaptation of echinoderms remains limited (Chen et al. 2022; Okanishi et al. 2020; Stöhr and Segonzac 2006; Zhang et al. 2022).

Although there have been fewer associated researches on ophiuroids in extensively vast deep-sea, where a comparable number of brittle star species has been recorded relative to shallow waters (Stöhr et al. 2012, 2025), this suggests a potentially high diversity in the deep sea (Christodoulou et al. 2020). Previous research suggests that ophiuroid species have likely undergone bidirectional evolution, involving transitions between deep-sea and shallow-water habitats (Bribiesca-Contreras et al. 2017; Thuy 2013). This demonstrates that the deep sea served as a significant site of origin for certain lineages of ophiuroids. However, the chronology of migration and dispersal events is unresolved, and the mechanisms underlying environmental adaptation and evolutionary change are still not well characterized. Many positive selection sites in mitochondrial genomes have also been reported in previous researches, which may also be linked to the adaptations to the deep-sea environment (Chen et al. 2022; Li et al. 2021; Na et al. 2024). Existing research has analyzed the adaptation mechanisms of cold-seep brittle stars in the South China Sea to their extreme environment (Chen et al. 2022; Li et al. 2021; Sun et al. 2023), but the adaptation mechanisms of hydrothermal vent brittle stars remain unexplored (Stöhr and Segonzac 2006; Okanishi et al. 2020).

To further explore phylogenetic relationships of Ophiuroidea and illustrate adaptative mechanism of species from deep-sea and hydrothermal vent environment, we newly sequenced mitochondrial genomes from four Ophiuroidea species inhabiting deep-sea reduced and

non-reduced environments. By combining these novel sequences with publicly available mitochondrial genomes from GenBank, we compiled a comprehensive dataset of 56 complete mitochondrial genomes representing 18 families of brittle stars. Our objectives were: (1) to reconstruct the phylogenetic relationship and ancestral state of Ophiuroidea based on the most comprehensive mitochondrial genomes; and (2) to assess the potential adaptive evolution of species to extreme environments, offering insights into the distinct evolutionary strategies employed by organisms inhabiting hydrothermal vents, cold seeps and non-reduced deep-sea habitats.

Materials and methods

Mitochondrial genomes sequencing, assembly and annotation

Genomic DNA was extracted from specimens preserved in 95% ethanol using the DNeasy Blood & Tissue Kit (QIAGEN, Germany) following the manufacturer's protocol. The extracted DNA were sequenced through the next-generation sequencing method, following Illumina's standard genomic DNA library preparation procedure. Paired-end libraries were constructed with insert sizes of approximately 400 bp. The qualified Illumina paired-end library (2 × 150 bp) was used for Illumina NovaSeq 6000 platform sequencing (Shanghai BIOZERON Co., Ltd.). The raw reads were filtered by fastp 0.24.0 (Chen et al. 2018) (Suppl. material 1: table S1), and clean reads were *de novo* assembled using NOVOPlasty 4.3.1 (Dierckxsens et al. 2017), obtaining four circular complete mitogenomes. Mitogenome annotations were performed via the Galaxy webserver MITOS2 toolset (https://usegalaxy.eu/). The boundaries of the PCGs, rRNAs and tRNAs were further manually determined by aligning with reference data through Geneious Prime 2024 software (Biomatters, Auckland, New Zealand). To describe the nucleotide composition of these four mitochondrial genomes, AT%, GC%, AT-skew and GC-skew were calculated by MEGA 11 (Caspermeyer 2018). The codon usage of the 13 PCGs was also calculated by MEGA 11 (Caspermeyer 2018). The complete mitogenome sequences were submitted in GenBank with the accession numbers of PV245937, PV295185, PV387752, and PV387751.

Phylogenetic analysis

Four newly sequenced deep-sea brittle stars (*Ophioctenella acies*, *Ophiura* cf. *irrorata*, *Ophiactis profundi*, and *Ophiocreas nudusoralis*), representing three ophiuroid orders, were included to improve the representation of deep-sea taxa in the phylogenetic analysis. Notably, this study reports the first complete mitochondrial genome of an ophiuroid species from a hydrothermal vent. Together with 52 ophiuroid mitochondrial genomes retrieved from NCBI, a total of 56 mitogenomes were used for phylogenetic reconstruction, with two asteroid mitochondrial genomes included as outgroups. The MUSCLE algorithm (Edgar 2004) was applied to align the amino acid sequences of the 13 PCGs. After alignment, ambiguously aligned regions were trimmed using TrimAl v1.4 (Capella-Gutiérrez et al. 2009) to ensure high-quality data for subsequent analysis. The IQ-TREE web server (Nguyen et al. 2015) (http://iqtree.cibiv.univie.ac.at/) was utilized for maximum likelihood (ML) analysis with the default settings, employing Bayesian information criterion to select the best models for each gene. RAxML v8.2.13 (Stamatakis 2014) was also used for generating the ML phylogenetic tree, with the model as GTR+CAT. MrBayes 3.2.7 (Ronquist and Huelsenbeck 2003) was employed to generate Bayesian inference (BI), under the mixed models, with mcmc nchains = 1, ngen = 300,000 sump burnin = 250, and sump burnin = 25,000. Based on the ML phylogenetic tree by IQ-TREE web server, we used branch model (model = 2) from PAML 4.10.7 package (Yang 2007) to analyze the evolutionary rate by estimating the non-synonymous substitution rate and the synonymous substitution rate (dn/ds).

Estimation of species divergence time

BEAST v1.10.4 (Suchard et al. 2018) was employed to estimate the timing of internal ancestral nodes, with calibrated time points provided in Suppl. material 1: table S2. We used 7 fossil-based node minimum constraints, spread across the major lineages (O'Hara et al. 2014; O'Hara et al. 2017). About the MCMC options, the length of chain was set as 300,000,000. The clock type was an uncorrelated relaxed clock. The substitution model and site heterogeneity model were Blosum62 + gamma. The priors of ucld. mean and ucld. stdev were set as uniform. In order to check the convergence of the runs, Tracer v1.7.1 (Rambaut et al. 2018) was used for examining the ESS of parameters. The initial 10% of generations were excluded as burn in. TreeAnnotator from BEAST package was utilized to summarize the node ages and the 95% highest posterior densities (HPD). The data of temperature and $\delta^{34}S$ we used for analysis were obtained from the previous studies, for reconstructing the historical dynamic change of global marine geochemistry (Etienne et al. 2012; Prokoph et al. 2008).

Ancestral state reconstruction

To assign rearrangements to the edges of the ML phylogenetic tree given by IQ-TREE web server and reconstruct ancestral gene orders at its inner nodes, these mitochondrial gene orders were compared with TreeREx 1.85 (Bernt et al. 2008). The gene orders of 37 mitochondrial genes from the 56 ophiuroids species and the outgroups were analyzed. One of the species (*Ophiocten ludwigi*)

was modified after downloading from NCBI. Upon alignment and re-annotation, we determined that its two rRNA genes were located on the negative strand, contrary to the original information provided on NCBI (Matsuo 2022). The results were visualized by Graphiviz 12.2.1 (Gansner and North 2000). The water depth of species in this study was collected and listed in Suppl. material 1: table S3. To compare the changes in the habitats of ancestral node more intuitively, we used the rerooting Method (Revell 2024) analysis of the R package phytools, with the model 'ADR'. The depth intervals were discretized as 0 to 200 m, 200 to 800 m, and 800 to 3500 m (O'Hara et al. 2017; Watling et al. 2013) for this study, based on the ML phylogenetic tree provided by IQ-TREE web server.

Positive selection analysis

To evaluate the variation in selective pressure of species from extreme environments (deep sea, hydrothermal vents, and cold seeps), positive selection analysis was conducted by using the CODEML program from PAML 4.10.7 package (Yang 2007), with the ML phylogenetic tree generated by IQ-TREE serving as the tree topology. The branch models, including one-ratio (model = 0), two-ratio (model = 2; assume different ω ratio (ω = dn/ds) between foreground branches and background branches) and free-ratio (model = 1; assume different ω ratio between every lineage), were applied to analyze the difference of selective pressure between different branches. The Branch-site model was utilized to detect whether the positive selections occurred in the foreground lineages during the evolution. Likelihood ratio tests (LRTs) were conducted to determine which kind of model was preferred to be used. If the LRTs were significant, Bayesian posterior probabilities of positively selected sites (with a posterior probability > 0.95) were calculated using Bayes Empirical Bayes (BEB). To compare the evolutionary rates between species from extreme environments, non-synonymous to synonymous rate ratio (ω = dn/ds) of 13 PCGs were calculated by two-ratio model implemented in the PAML 4.10.7 package.

Results and discussion

The characteristics of mitochondrial genomes

Key features of the four newly sequenced mitochondrial genomes are summarized in Suppl. material 1: table S3. These mitochondrial genomes consist of 37 genes, and their total lengths are as follows: *Ophioctenella acies* (16,290 bp), *Ophiura* cf. *irrorata* (16,210 bp), *Ophiactis profundi* (15,850 bp) and *Ophiocreas nudusoralis* (16,326 bp). The nucleotide compositions of the whole mitogenomes, PCGs gene and rRNA genes are provided in Suppl. material 1: table S5. Notably, the A+T contents across the four orders are highly variable, ranging from 58.62% to 66.76% in Amphilepidida, from 62.18% to 74.62% in Ophiacanthida, from 63.59% to 69.37% in Ophiurida and from 64.43% to 73.66% in Euryalida (Suppl. material 1: table S5). The A+T contents of the four new mitochondrial genomes fall within the respective variation range of their orders. The A+T content in *O. profundi* (59.05%) is distinctly lower than the other three species (68.01% in *O.* cf. *irrorata*., 66.21% in *O. acies* and 68.19% in *O. nudusoralis*). There were significant differences in AT-skew and GC-skew between different orders (Fig. 1). The AT-skew values of the four species are positive, and the GC-skew values are negative (Fig. 1, Suppl. material 1: table S5). Interestingly, the AT-skew values of *O.* cf. *irrorata* and *O. acies* are higher than other species in Ophiurida, which are typically, except *Ophioplinthus breevirima* and *Ophiomusium* sp. with slightly lower positive AT-skew values (Suppl. material 1: table S5).

Among the 13 PCGs (Suppl. material 1: table S5), the majority of start codons are ATG, with several exceptions observed, such as GTG in COX1 of *O. profundi*, ATT in ND5 of *O. profundi* and COX1 & ND1 of *O. nudysoralis*. Most genes terminate with complete stop codons (TAG or TAA), although truncated stop codons are occasionally found in ND2 (TA for *O. profundi*, TA for *O. nudysoralis*), ND4L (T for *O. nudysoralis*), CYTB (T for *O. profundi*). Compared with TAG, TAA is more frequently used in the 13 PCGs across these mitogenomes. The codon usage and relative synonymous codon usage (RSCU) values for the PCGs (excluding stop codons) are shown in Fig. 2. Among the 13 PCGs of these four species, leucine is the most frequently used amino acid (14.46% in *O. acies*, 14.29% in *O.* cf. *irrorata*, 15.99% in *O. nudusoralis*, and 15.57% in *O. profundi*), while cysteine is the least (0.95% in *O. acies*, 0.90% in *O.* cf. *irrorata*, 0.93% in *O. nudusoralis*, and 1.24% in *O. profundi*). The RSCU values are used to identify the seven most commonly used codons of the four species, highlighting clearly A + T bias at their third codon position.

Phylogenetic relationship of Ophiuroidea

Phylogenetic trees constructed through three different methods in this study showed similar topologies with minus differences. In the ML tree generated by IQtree, *Ophiocten ludwigi* was the sister clade of *Ophiura albida*, whereas it clustered with the other three species (*O. acies*, *O. sarsii* and *O. lutkeni*) in the trees generated by RAxML and MrBayes (Fig. 3). *Amphiura* sp. (OP273954) was grouped with *Amphipholis squamata* and *A. digitula* in the ML trees, but was clustered with *A.* sp. (MN296491) and *Amphiura sinicola* in the BI tree. All these three phylogenetic trees in this study confirm the four orders as monophyletic clades (Fig. 3),

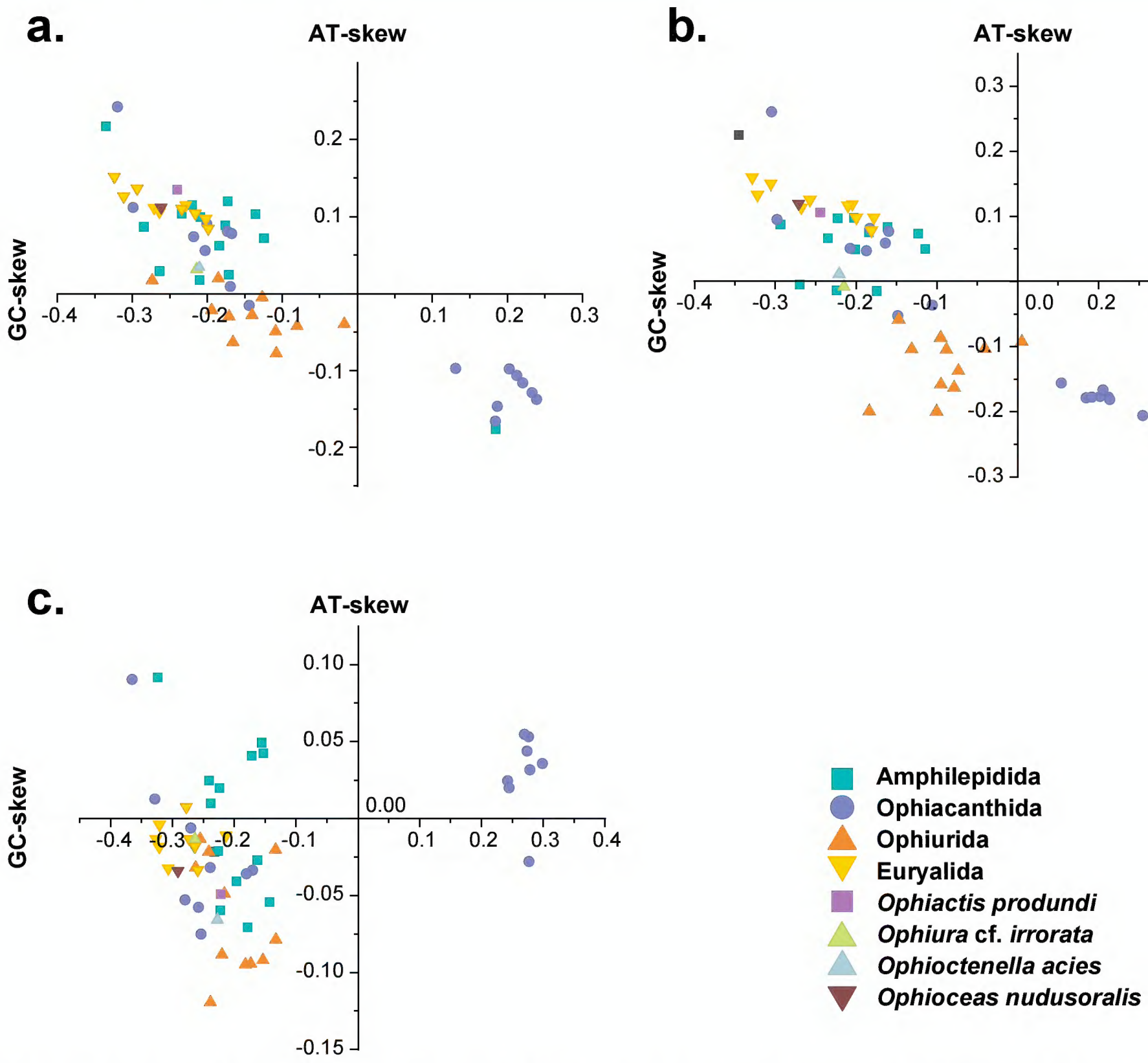

Figure 1. AT-skew and GC-skew values of Ophiuroidea. **a.** The whole mitochondrial genomes; **b.** 13 PCGs, and **c.** Two rRNAs.

consistent with the current classification system (O'Hara et al. 2017). The two major clades, Ophintegrida and Euryophiurida, were consistently supported by previous phylogenetic analysis based on mitochondrial genomes, as well as Ophiurida and Euryalida (Chen et al. 2022; Galaska et al. 2019; Lee et al. 2019; Na et al. 2024; Sun et al. 2023). However, the monophyly of Amphilepidida and Ophiacanthida has remained controversial. The two species (*Ophioceres incipiens* and *Ophioplocus japonicus*) of Hemieuryalidae were clustered with Ophiacanthids rather than Amphilepidida (Lee et al. 2019; Na et al. 2024; Sun et al. 2023), whereas in some other cases, *Ophiarachnella gorgonia*, *Ophiomastix mixta* and *Ophiocamax drygalskii* were clustered with Amphilepidida (Na et al. 2024). Only Chen et al. (2022) and Na et al. (2024) provided trees support the monophyly of Amphilepidida and Ophiacanthida using amino acid sequences, however, the support values on key nodes are modest, suggesting that further studies are needed to confirm theses nodes.

At lower taxonomic levels, the phylogenetic relationships within Ophiurida appeared contentious as previous study (Chen et al. 2022; Na et al. 2024; O'Hara et al. 2017). Unlike the topology recovered by O'Hara et al. (2017), our results suggested that *Ophionotus victoriae* has a closer relationship with Ophiopyrgidae rather than Ophiuridae. Similar contradictions have also been noted in previous mitochondrial genome-based phylogenies (Chen et al. 2022; Na et al. 2024). Minus conflicts of phylogenetic relationships within the genus *Ophiura* were also observed compared with earlier findings (O'Hara et al. 2017). *Ophiura albida* was the sister clade of *O. ludwigi* in this study, but was the sister clade of *O. acies* (O'Hara et al. 2017). The phylogenetic relationships of species from the two families Ophiuridae and Ophiopyrgidae were extremely complicated (O'Hara et al. 2017), especially given that a large number of species of *Ophiura*, which is one of the most diverse genera of Ophiuridae, were transferred to Ophiopyrgidae mostly based on molecular data.

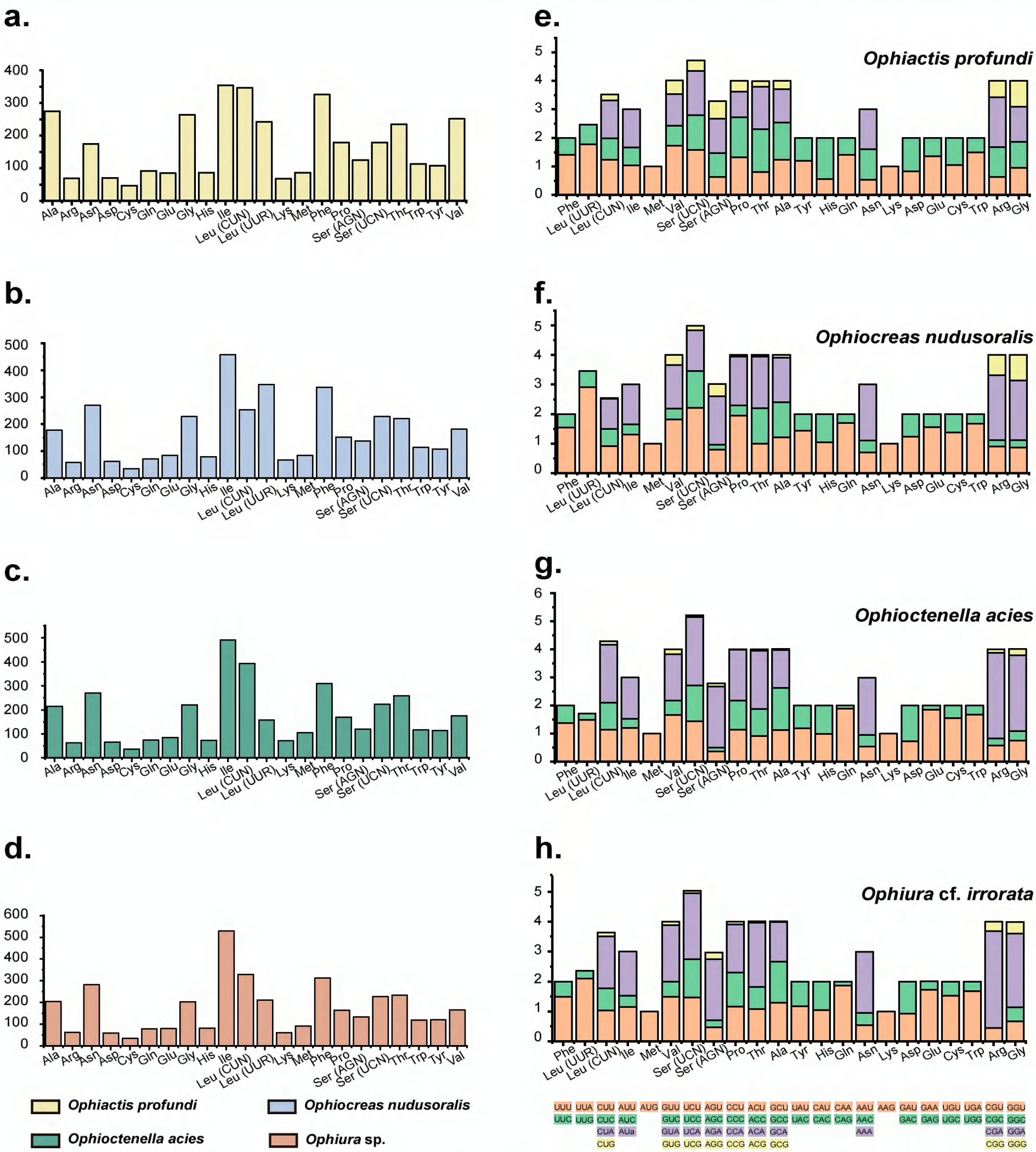
a.
b.
c.
d.
e.
f.
g.
h.
Ophiactis profundi
Ophiocreas nudusoralis
Ophioctenella acies
Ophiura sp.
Ophiura cf. irrorata
Ala Arg Asn Asp Cys Gln Glu Gly His Ile Leu (CUN) Leu (UUR) Lys Met Phe Pro Ser (AGN) Ser (UCN) Thr Trp Tyr Val
Phe Leu (UUR) Leu (CUN) Ile Met Val Ser (UCN) Ser (AGN) Pro Thr Ala Tyr His Gln Asn Lys Asp Glu Cys Trp Arg Gly
UUU UUA CUU AUU AUG GUU UCU AGU CCU ACU GCU UAU CAU CAA AAU AAG GAU GAA UGU UGA CGU GGU
UUC UUG CUC AUC GUC UCC AGC CCC ACC GCC UAC CAC CAG AAC GAC GAG UGC UGG CGC GGC
CUA AUa GUA UCA AGA CCA ACA GCA AAA CGA GGA
CUG GUG UCG AGG CCG ACG GCG CGG GGG

Figure 2. Codon usage (**a–d**) with Different colors representing different species and the relative synonymous codon usage (RSCU) (**e–h**) of the four newly sequenced species

An integrated review through both morphological and molecular analysis is emergently needed. The phylogenetic relationships among the three families within Euryalida in our research are consistent with previous studies (Na et al. 2024; Okanishi and Fujita 2013), showing that Asteronychidae is clustered with Gorgonocephalidae rather than being positioned as a basal clade of Euryalida (O'Hara et al. 2017). Only one species representing Asteronychidae was included in our analysis; further sampling efforts of Asteronychidae may provide better understanding on phylogeny of the three euryalid families. With the inclusion of more mitochondrial genomic data, our phylogenetic trees of Ophiuroidea were notably improved compared with previous studies(Chen et al. 2022; Galaska et al. 2019; Lee et al. 2019; Na et al. 2024; Sun et al. 2023), supporting the monophyly of the four major orders, covers the monophyly of all four orders, reaffirming the academic significance of mitochondrial genomes and importance of stronger sampling efforts in phylogenetic analysis.

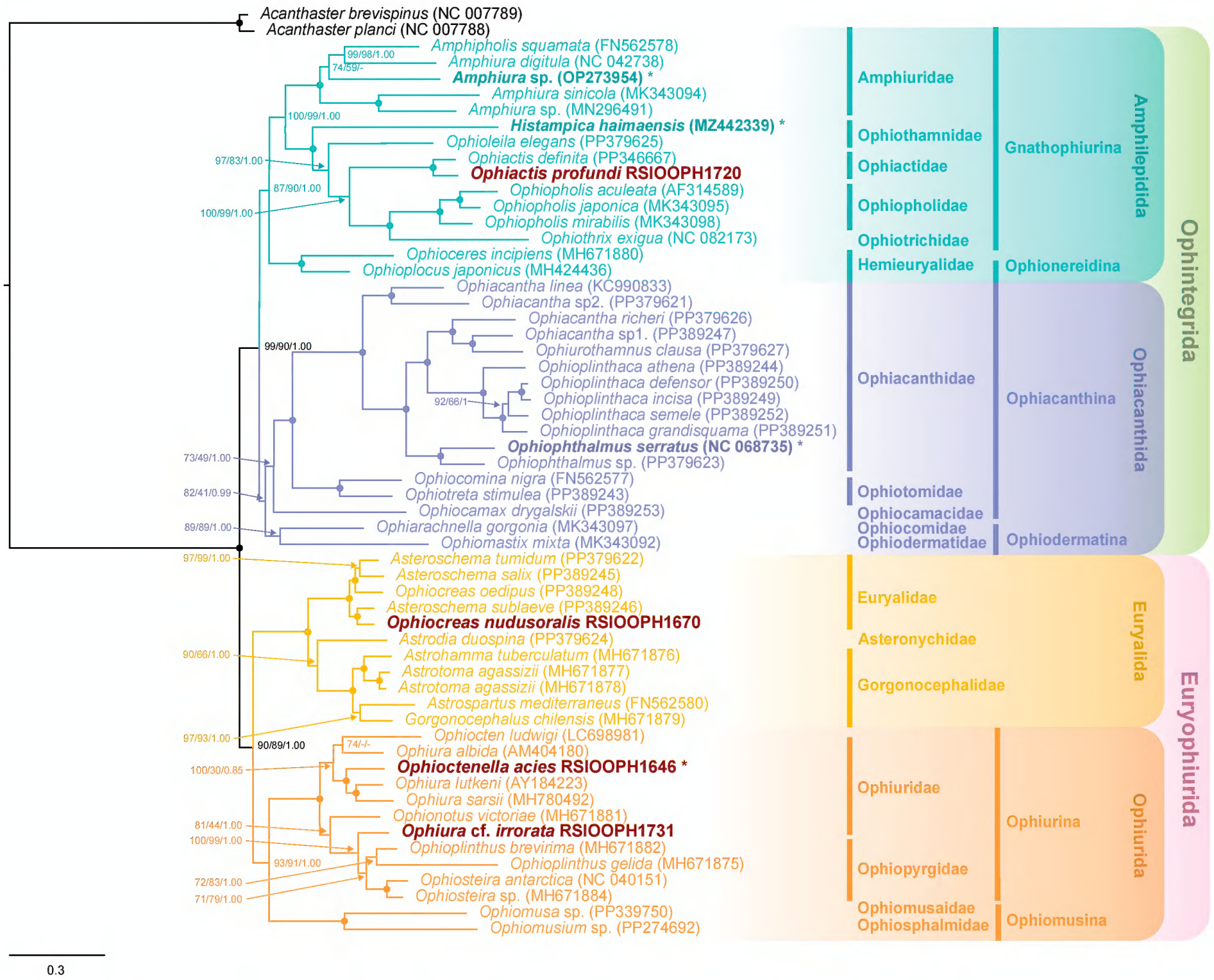

Figure 3. ML phylogenetic trees of Ophiuroidea inferred from the amino acid databases using IQ-TREE. Numbers on nodes are bootstrap values and posterior probability (left from ML phylogenetic tree of IQtree; middle from ML phylogenetic tree of RAxML; right from BI phylogenetic tree of Mrbayes). Species in chemosynthetic habitats are marked in bold with asterisks.

Divergence time of Ophiuroidea

The details of specie divergence time are shown in Fig. 4. These four newly sequenced species diverged between 60 to 25 Ma, during the Paleogene, Cenozoic Era (66 Ma to present) (Cohen et al. 2024). More detailed, two (*O. profundi* and *O. nudysoralis*) of them diverged during the Oligocene, and two (*O.* cf. *irrorata* and *O. acies*)during the Paleocene. Among the four species, *O. acies* diverged earliest, approximately 59.39 Ma. *Ophiura.* cf. *irrorata* followed with a divergence around 57.79 Ma ago, while *O. profundi* diverged about 29.63 Ma ago. *O. nudysoralis* exhibited the most recent divergence in these four species, occurring around 25.13 Ma. The most common ancestor of Ophiuroidea originated around the boundary between Permian and Triassic (about 255.24 Ma), corresponding to the Permian-Triassic mass extinction event (Stanley 2016). Among the four major orders, Ophiacanthida and Amphilepidida radiated at the Triassic (244.38 Ma and 227.23 Ma, respectively), Ophiurida radiated during the Jurassic (160.27 Ma), while Euryalida radiated more recently at the Cretaceous (106.34 Ma). These divergence time estimates are generally consistent with previous studies (O'Hara et al. 2017; Sun et al. 2023).

Integrating the ancestral biogeographic distribution reconstructions from the rerootingMethod (Fig. 4) revealed divergent evolutionary histories among ophiuroid lineages. Ophiacanthids first occurred and diversified in the deep sea during the Early Triassic, which is consistent with the fossil evidence (Thuy 2013), suggesting that Ophiacanthidae more likely originated in the deep sea. Thuy (2013) indicated that Ophiacanthidae temporarily invaded shallow-water environments from the deep sea during the Jurassic. Similar to the Ophiacanthids, Euryalida was also more likely to have originated in the deep sea and underwent multiple invasions from the deep sea to shallow waters. Deep-sea species from Amphilepidida diverged from their shallow water congeners in the Jurassic. Deep-sea species from Ophiomusina were found diverged from their ancestor in the early Jurassic, while the other deep-sea species diverged in the Cretaceous. Bidirectional invasions, from shallow to deep seas or vice versa, may be

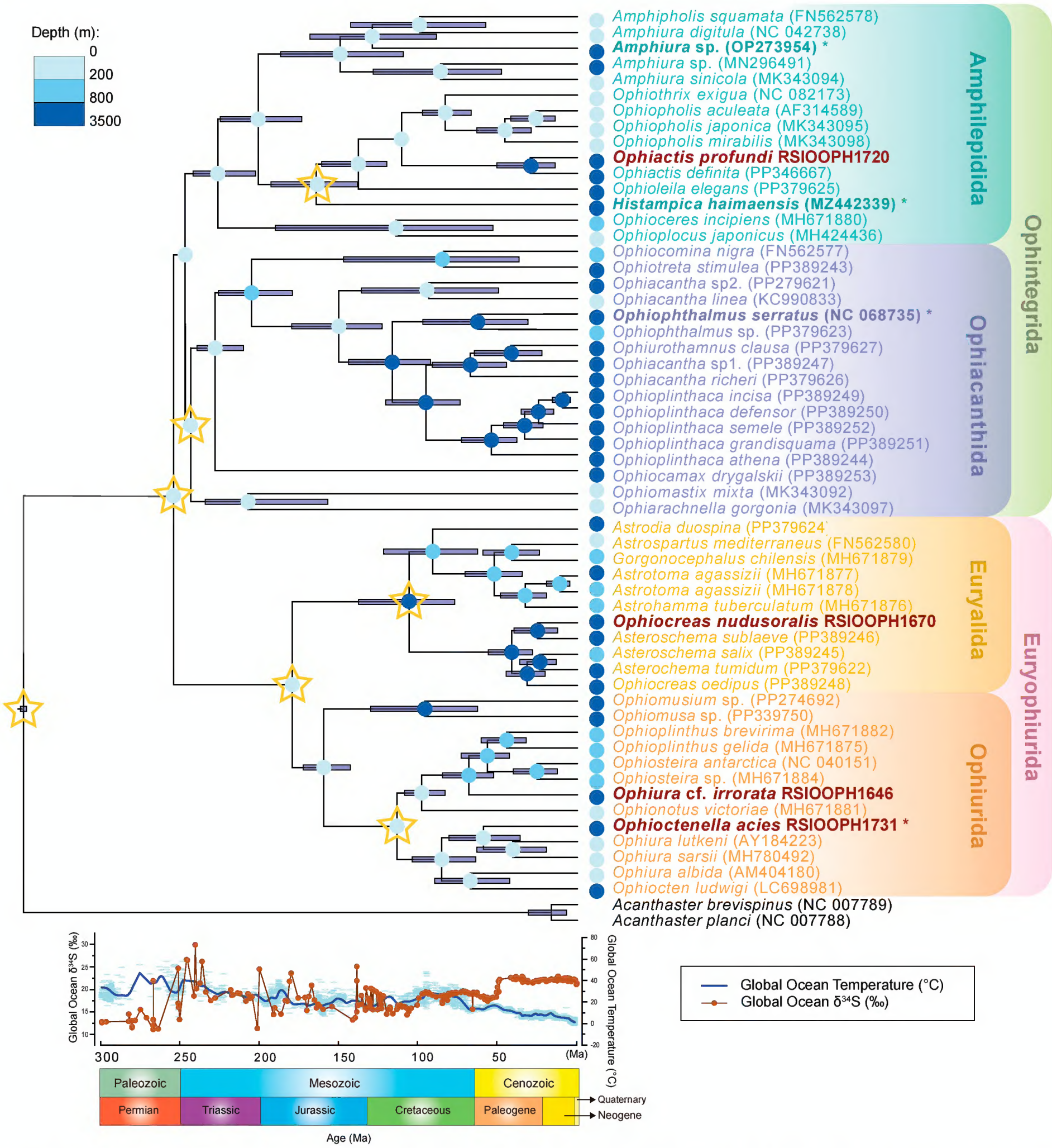

Figure 4. Divergence time chronogram of Ophiuroidea estimated by BEAST. The 95% confidence intervals for each node are marked in purple bars. The fossil calibration points are marked with yellow pentagrams. Ancestral nodes' water depth was reconstructed by the rerootingMethod from R package phytools. Chemosynthetic habitat species are indicated in bold with asterisks. Global ocean temperatures were shown with blue dots, and $\delta^{34}S$ (‰) were displayed by a brown solid line with brown elliptic points.

associated with geological events during the Late Jurassic to Early Cretaceous (Araripe et al. 2021; Huber et al. 2002; Ma et al. 2025; Melo et al. 2020; Michels et al. 2018; Ray et al. 2019). During this period, plate tectonics and the formation of new marine basins facilitated the migration and dispersal of marine organisms (Araripe et al. 2021; Ma et al. 2025; Melo et al. 2020; Michels et al. 2018). Concurrently, rising deep-sea temperatures (Huber et al. 2002) reduced the thermal gradient between surface and deep waters, and a relatively significant rise in sea level (Ray et al. 2019) drove the adaptation of Ophiuroidea species to deep-sea environments, promoting biological exchange between shallow and deep-sea ecosystems. Subsequently, intensified ocean stratification due to anoxic events, among other factors, led to the differentiation of these species. In this study, those divergence events between deep-sea and shallow-water species found at the mid-Cretaceous may be attributed to distinctive repeated oceanic anoxic events (OAEs) and the relative warm geological intervals (Matsumoto et al. 2022).

In addition, chemosynthetic ecosystem colonization may be further linked to marine sulfate fluctuations, which can influence the chemosynthetic habitat species by directly affecting the food chain (Kiel 2015). Among the four species from the chemosynthetic ecosystem, *Histampica haimaensis* is the first cold-seep species to diverge at the mid-Jurassic (164.98 Ma), *Amphiura* sp. diverged at the early Cretaceous (126.62 Ma), *Ophiophthalmus serratus* and *Ophioctenella acies* diverged from their congeners at the early Paleogene (62.98 Ma and 59.39 Ma, respectively). These divergence time estimates are similar to previous studies (O'Hara et al. 2017; Sun et al. 2023). Among them, three species of the four chemosynthetic habitat species experienced significant fluctuations in $\delta^{34}S$ (‰) just prior to their differentiation (Fig. 4).

Adaptive evolution analysis of Ophiuroidea

The mitochondrial gene orders of the four newly sequenced species were consistent with their congeneric taxa (Chen et al. 2022; Li et al. 2021; Na et al. 2024), with the exception of *Ophiura* cf. *irrorata*, which exhibited a gene order resembling that of its closely related species (e.g. *Ophiosteira antarctica* and *Ophiosteira* sp.), rather than other species in *Ophiura*. The three cold-seep species exhibited variable gene rearrangements compared to their closely related species; *Histampica haimaensis* underwent extensive rearrangements including multiple inversions and a TDRL event, *Ophiophthalmus serratus* have undergone a duplication of tRNA M, and *Amphiura*. sp. (OP273954) only exhibited a single tRNA gene transposition of tRNA M (Fig. 5). However, no gene rearrangement event was observed from the hydrothermal vent species *Ophioctenella acies*. The LRT analysis showed that the two-ratio branch model is significantly better than the one-ratio model using *Ophioctenella acies* as foreground for ATP8 and ND4. Significant differences between the two models were also found for COX3 and ND4 when using *Ophiophthalmus serratus* as foreground, for COX1 and COX3 when using *Histampica haimaensis* as foreground (Suppl. material 1: table S6). Positive selection signals were detected from the three cold-seep species in this study by branch site model, one for *O. serratus* (ATP 6), two for *Amphiura*. sp. (ATP 8 and ND 2), and two for *H. haimaensis* (COX 1 and COX 2) (Fig. 5). However, no positive signal was found from *O. acies*. Among the four species, *O. serratus* showed relatively higher nucleotide substitute rates than the other three species, while *O. acies* exhibited the lowest nucleotide substitute rates (Fig. 6).

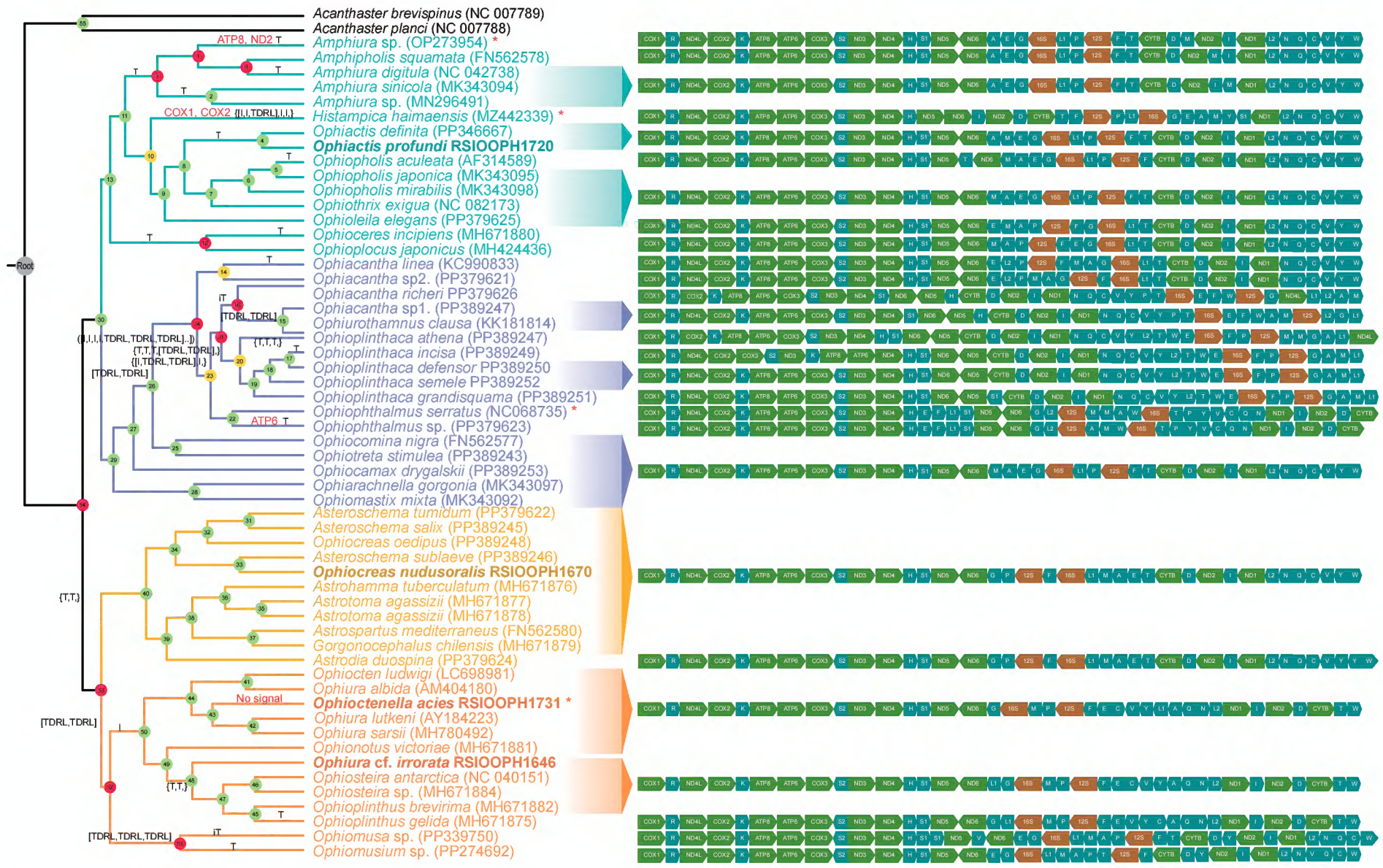

Figure 5. Possible scenario of mitochondrial gene rearrangement of 37 genes in Ophiuroidea. Gene orders at the node were estimated using TreeREx based on the phylogenetic relationships shown in Fig. 3. The rearrangements on the branches are denoted as "T" for transposition, "TDRL" for tandem duplication-random-loss events, "I" for inversion, and "iT" for inversion and transposition (remote inversion) events. Node numbers 0 to 55 are assigned to each node. Consistently reconstructed nodes are indicated by green circles; 1-consistent reconstructed nodes are indicated by yellow circles; and nodes reconstructed using the fallback method are indicated by red circles. Species in chemosynthetic habitats are marked with asterisks. Positive selection results are displayed in red font.

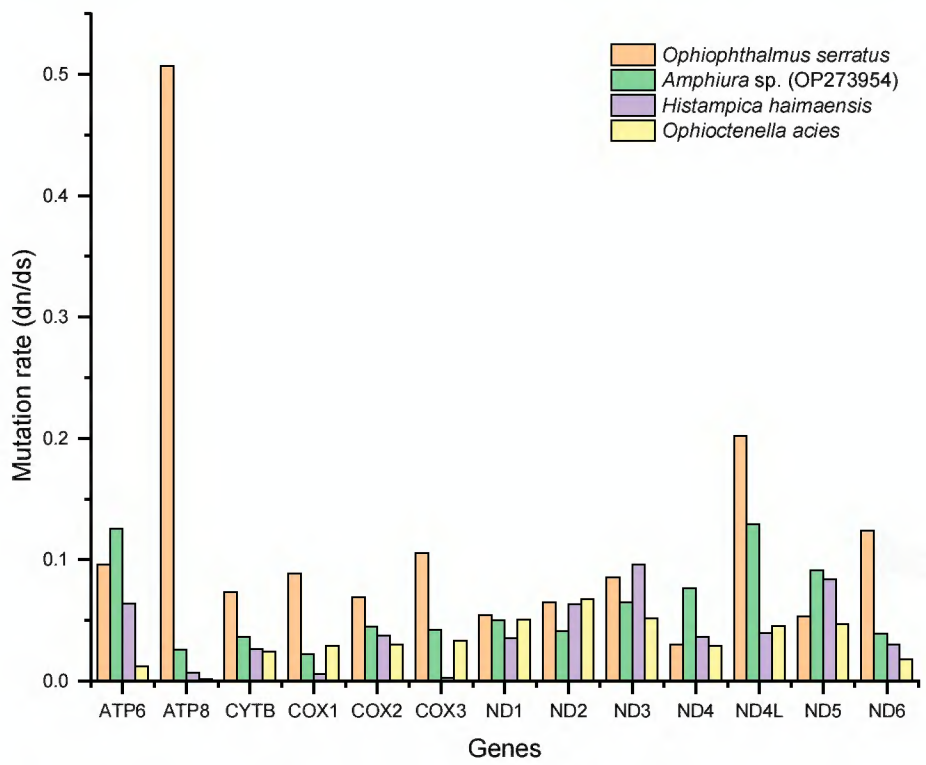

Figure 6. Mutation rates of the four chemosynthetic species estimated by PAML. Gene order of each mitogenome was displayed on the right of the Figure.

As far as we know, extreme environments can influence the functions of mitochondrial genes, resulting in mitochondrial genome order rearrangements and the emergence of positive selections (da Fonseca et al. 2008; Garvin et al. 2015; Sun et al. 2019; Welch et al. 2014). In the previous study, Chen et al. (2022) revealed gene rearrangement and positive selection signals from the three cold-seep species, which was also supported by our results, suggesting that the functions of mitochondrial genes may be shaped by adaptive mechanisms to the extreme conditions. However, no gene rearrangements or positive selection signals were identified in the newly sequenced hydrothermal vent species *O. acies*, despite its starkly contrasting habitat compared to its sister species. Compared with the other three cold-seep species, its lower nucleotide substitution rates for most of the 13 PCGs (Fig. 6) also demonstrated that this branch is relatively conserved and may have undergone extensive purifying selection. Although numerous studies support the idea that extreme environments in hydrothermal vents tend to promote positive selection in mitochondrial genomes (Yang et al. 2019; Zhang et al. 2017; Zhang et al. 2021), some researches also suggested that species may adapt to extreme environmental conditions through purifying selection by reducing the accumulation of harmful mutations (Meiklejohn et al. 2007; Vieira et al. 2024).

Conclusions

In this study, we sequenced and characterized mitochondrial genomes of four deep-sea ophiuroid species, including the first mitochondrial genome reported from a hydrothermal vent species. Their lengths and nucleotide composition fell into the variation of Ophiuroidea. Combining these with existing GenBank data, we analyzed 56 complete mitogenomes of Ophiuroidea spanning 18 families. Phylogenetic analysis based on 13 PCGs supported the monophyly of the two superorders (Ophintegrida and Euryophiurida), four orders (Euryalida, Ophiurida, Amphilepidida and Ophiacanthida), and most families within this class, consistent with current systematics of Ophiuroidea. Support values of phylogenetic trees on major nodes were higher than in previous studies. The divergence time estimates indicated that Ophiuroidea originated around the boundary between Permian and Triassic, and Ophiacanthida and Amphilepidida originated earlier than Ophiurida and Euryalida. Most deep-sea species diverged from their shallow water congeners during the Jurassic and Cretaceous. Neither gene rearrangement events nor positive selective sites were found in the hydrothermal vent species; on the contrary, they were uncovered from the three cold-seep species, suggesting the hydrothermal vent species may have undergone strong purifying selection or have a low mutation rate.

Acknowledgements

We appreciate the crews of R/V *SHENHAIYIHAO*, as well as the operation teams of HOV *JIAOLONG* for their invaluable help in collecting the samples used in this study. We thank the anonymous reviewers for their constructive suggestions. This work was supported by the National Key R&D Program of China (2025YFE0210800 and 2023YFC2812903), the National Natural Science Foundation of China (42076135) and the UN Ocean Decade Programme "Digital DEPTH".

References

Araripe RC, Oliveira DH, Tomé ME, Moura de Mello R, Barreto AMF (2021) Foraminifera and Ostracoda from the Lower Cretaceous (Aptian–lower Albian) romualdo formation, Araripe basin, northeast Brazil: Paleoenvironmental inferences. Cretaceous Research 122. https://doi.org/10.1016/j.cretres.2021.104766

Bebianno MJ, Cardoso C, Gomes T, Blasco J, Santos RS, Colaco A (2018) Metal interactions between the polychaete Branchipolynoe seepensis and the mussel Bathymodiolus azoricus from Mid-Atlantic-Ridge hydrothermal vent fields. Marine Environmental Research 135: 70–81. https://doi.org/10.1016/j.marenvres.2018.01.017

Bernt MB, Merkle DM, Middendorf M (2008) An algorithm for inferring mitogenome rearrangements in a phylogenetic tree. Comparative Genomics, 143–157. https://doi.org/10.1007/978-3-540-87989-3_11

Boore JL, Lavrov DV, Brown WM (1998) Gene translocation links insects and crustaceans. Nature 392: 667–668. https://doi.org/10.1038/33577

Bribiesca-Contreras G, Verbruggen H, Hugall AF, O'Hara TD (2017) The importance of offshore origination revealed through ophiuroid phylogenomics. Proceedings of the Royal Society B: Biological Sciences 284(1858). https://doi.org/10.1098/rspb.2017.0160

Campoy AN, Rivadeneira MM, Hernandez CE, Meade A, Venditti C (2023) Deep-sea origin and depth colonization associated with phenotypic innovations in scleractinian corals. Nature Communication 14(1): 7458. https://doi.org/10.1038/s41467-023-43287-y

Capella-Gutiérrez S, Silla-Martinez JM, Gabaldon T (2009) trimAl: a tool for automated alignment trimming in large-scale phylogenetic analyses. Bioinformatics 25(15): 1972–1973. https://doi.org/10.1093/bioinformatics/btp348

Caspermeyer J (2018) MEGA Software Celebrates Silver Anniversary. Molecular Biology and Evolution 35(6): 1558–1560. https://doi.org/10.1093/molbev/msy098

Chen S, Zhou Y, Chen Y, Gu J (2018) fastp: an ultra-fast all-in-one FASTQ preprocessor. Bioinformatics 34(17): i884–i890. https://doi.org/10.1093/bioinformatics/bty560

Chen Z, Ma S, Qin G, Qu M, Zhang B, Lin Q (2022) Strategy of micro-environmental adaptation to cold seep among different brittle stars' colonization. Frontiers in Ecology and Evolution 10. https://doi.org/10.3389/fevo.2022.1027139

Choi H, Yu OH, Eyun SI (2025) Evolutionary insights into adaptation of hemocyanins from deep-sea hydrothermal vent shrimps. Marine Pollution Bulletin 215: 117872. https://doi.org/10.1016/j.marpolbul.2025.117872

Christodoulou M, O'Hara T, Hugall AF, Khodami S, Rodrigues CF, Hilario A, Vink A, Arbizu PM (2020) Unexpected high abyssal ophiuroid diversity in polymetallic nodule fields of the northeast Pacific Ocean and implications for conservation. Biogeosciences 17(7): 1845-1876. https://doi.org/10.5194/bg-17-1845-2020

Cohen KM, Harper DAT, Gibbard PL (2024) ICS International Chronostratigraphic Chart 2025/Dec. www.stratigraphy.org [March 11, 2025]

da Fonseca RR, Johnson WE, O'Brien SJ, Ramos MJ, Antunes A (2008) The adaptive evolution of the mammalian mitochondrial genome. BMC Genomics 9: 119. https://doi.org/10.1186/1471-2164-9-119

Dierckxsens N, Mardulyn P, Smits G (2017) NOVOPlasty: de novo assembly of organelle genomes from whole genome data. Nucleic acids research 45(4): e18. https://doi.org/10.1093/nar/gkw955

Edgar RC (2004) MUSCLE: multiple sequence alignment with high accuracy and high throughput. Nucleic acids research 32(5): 1792–1797. https://doi.org/10.1093/nar/gkh340

Elson JL, Lightowlers RN (2006) Mitochondrial DNA clonality in the dock: can surveillance swing the case? TRENDS in Genetics 22(11): 603–607. https://doi.org/10.1016/j.tig.2006.09.004

Emson RH, Mladenov PV, Barrow K (1991) The feeding mechanism of the basket star Gorgonocephalus arcticus. Canadian Journal of Zoology 69(2): 449–455. https://doi.org/10.1139/z91-070

Etienne RS, Haegeman B, Stadler T, Aze T, Pearson PN, Purvis A, Phillimore AB (2012) Diversity-dependence brings molecular phylogenies closer to agreement with the fossil record. Proceedings. Biological sciences 279(1732): 1300–1309. https://doi.org/10.1098/rspb.2011.1439

Fell HB (1960) Synoptic keys to the genera of Ophiuroidea. Zoology Publications from Victoria University of Wellington 26: 1–44.

Fratt DB, Dearborn JH (1984) Feeding biology of the Antarctic brittle star Ophionotus *victoriae* (Echinodermata: Ophiuroidea). Polar Biology 3: 127–139. https://doi.org/10.1007/bf00442644

Galaska MP, Li Y, Kocot KM, Mahon AR, Halanych KM (2019) Conservation of mitochondrial genome arrangements in brittle stars (Echinodermata, Ophiuroidea). Molecular Phylogenetics and Evolution 130: 115–120. https://doi.org/10.1016/j.ympev.2018.10.002

Galaska MP, Sands CJ, Santos SR, Mahon AR, Halanych KM (2017) Geographic structure in the Southern Ocean circumpolar brittle star Ophionotus victoriae (Ophiuridae) revealed from mtDNA and single-nucleotide polymorphism data. Ecology and Evolution 7(2): 475–485. https://doi.org/10.1002/ece3.2617

Gansner ER, North SC (2000) An open graph visualization system and its applications to software engineering. Software: Practice and Experience 30(11): 1203–1233. https://doi.org/10.1002/1097-024x(200009)30:11<1203::aid-spe338>3.0.co;2-n;2-n

Garvin MR, Thorgaard GH, Narum SR (2015) Differential Expression of Genes that Control Respiration Contribute to Thermal Adaptation in Redband Trout (Oncorhynchus mykiss gairdneri). Genome biology and evolution 7(6): 1404–1414. https://doi.org/10.1093/gbe/evv078

Gissi C, Iannelli F, Pesole G (2008) Evolution of the mitochondrial genome of Metazoa as exemplified by comparison of congeneric species. Heredity 101(4): 301–320. https://doi.org/10.1038/hdy.2008.62

Huber BT, Norris RD, MacLeod KG (2002) Deep-sea paleotemperature record of extreme warmth during the Cretaceous. Geology 30(2): 123–126. https://doi.org/10.1130/0091-7613(2002)030<0123:d-sproe>2.0.co;2;2

Hui M, Cheng J, Sha Z (2018) Adaptation to the deep-sea hydrothermal vents and cold seeps: Insights from the transcriptomes of Alvinocaris longirostris in both environments. Deep-Sea Research Part I 135: 23–33. https://doi.org/10.1016/j.dsr.2018.03.014

Ip JC, Xu T, Sun J, Li R, Chen C, Lan Y, Han Z, Zhang H, Wei J, Wang H, Tao J, Cai Z, Qian PY, Qiu JW (2021) Host-Endosymbiont Genome Integration in a Deep-Sea Chemosymbiotic Clam. Molecular Biology and Evolution 38(2): 502–518. https://doi.org/10.1093/molbev/msaa241

Kiel S (2015) Did shifting seawater sulfate concentrations drive the evolution of deep-sea methane-seep ecosystems? Proceedings. Biological sciences 282(1804): 20142908. https://doi.org/10.1098/rspb.2014.2908

Lavrov DV, Lang BF (2005) Poriferan mtDNA and animal phylogeny based on mitochondrial gene arrangements. Systematic biology 54(4): 651–659. https://doi.org/10.1080/10635150500221044

Lee T, Bae YJ, Shin S (2019) Mitochondrial gene rearrangement and phylogenetic relationships in the Amphilepidida and Ophiacanthida (Echinodermata, Ophiuroidea). Marine Biology Research 15(1): 26–35. https://doi.org/10.1080/17451000.2019.1601226

Li Q, Li Y, Na J, Han X, Paterson GLJ, Liu K, Zhang D, Qiu J-W (2021) Description of a new species of *Histampica* (Ophiuroidea: Ophiothamnidae) from cold seeps in the South China Sea and analysis of its mitochondrial genome. Deep-Sea Research Part I, 178 pp. https://doi.org/10.1016/j.dsr.2021.103658

Li Y, Tassia MG, Waits DS, Bogantes VE, David KT, Halanych KM (2019) Genomic adaptations to chemosymbiosis in the deep-sea seep-dwelling tubeworm Lamellibrachia luymesi. BMC Biology 17(1): 91. https://doi.org/10.1186/s12915-019-0713-x

Ma J, Cury LF, Rumbelsperger AMB, Albrecht HL, Adams EW, Amthor JE, Cui X, Crémière A, Sato K, Bergmann KD, Summons RE (2025) Ecosystem changes after Early Cretaceous seawater intrusion into the proto-South Atlantic Ocean. Communications Earth & Environment 6(1). https://doi.org/10.1038/s43247-025-02029-2

Matsumoto H (1917) A monograph of Japanese Ophiuroidea, arranged according to a new classification. Journal of the College of Science, Imperial University of Tokyo, 38 pp.

Matsumoto H, Coccioni R, Frontalini F, Shirai K, Jovane L, Trindade R, Savian JF, Kuroda J (2022) Mid-Cretaceous marine Os isotope evidence for heterogeneous cause of oceanic anoxic events. Nature

Communication 13(1): 239. https://doi.org/10.1038/s41467-021-27817-0

Matsuo T (2022) Ophiocten ludwigi Octen_lud_01 mitochondrial DNA, nearly complete genome. https://www.ncbi.nlm.nih.gov/nuccore/LC698981 [October 10, 2024]

McMullin ER, Bergquist DC, Fisher CR (2000) Metazoans in extreme environments: Adaptations of hydrothermal vent and hydrocarbon seep fauna. Gravitational and space biology bulletin 13(2): 13–23.

Meiklejohn CD, Montooth KL, Rand DM (2007) Positive and negative selection on the mitochondrial genome. TRENDS in Genetics 23(6): 259–263. https://doi.org/10.1016/j.tig.2007.03.008

Melo RM, Guzman J, Almeida-Lima D, Piovesan EK, Neumann V, Sousa AJE (2020) New marine data and age accuracy of the Romualdo Formation, Araripe Basin, Brazil. Scientific Reports 10(1): 15779. https://doi.org/10.1038/s41598-020-72789-8

Michels FH, Souza PAd, Premaor E (2018) Aptian-Albian palynologic assemblages interbedded within salt deposits in the Espírito Santo Basin, eastern Brazil: Biostratigraphical and paleoenvironmental analysis. Marine and Petroleum Geology 91: 785–799. https://doi.org/10.1016/j.marpetgeo.2018.01.023

Mikkelsen NT, Kocot KM, Halanych KM (2018) Mitogenomics reveals phylogenetic relationships of caudofoveate aplacophoran molluscs. Molecular Phylogenetics and Evolution 127: 429–436. https://doi.org/10.1016/j.ympev.2018.04.031

Mladenov PV, Emson RH (1988) Density, size structure and reproductive characteristics of fissiparous brittle stars in algae and sponges: evidence for interpopulational variation in levels of sexual and asexual reproduction. Marine Ecology Progress Series 42: 181–194. https://doi.org/10.3354/meps042181

Na J, Zhang D, Cheng H, Yang J, Zhang R, Chen W, Wang C (2019) The complete mitochondrial genome of a deep sea ophiuroid of the genus *Amphiura* (Ophiuroidea: Amphiuridae). Mitochondrial DNA Part B 4(2): 3709–3710. https://doi.org/10.1080/23802359.2019.1679047

Na J, Zhou Y, Cheng H, Zhang R, Shen C, Lu B, Wang C, Zhang D (2024) Phylogenetic relationships and lineage-specific mitochondrial gene rearrangement in Ophiuroidea: insights from mitochondrial genomes. Frontiers in Marine Science 11. https://doi.org/10.3389/fmars.2024.1425922

Nguyen LT, Schmidt HA, von Haeseler A, Minh BQ (2015) IQ-TREE: a fast and effective stochastic algorithm for estimating maximum-likelihood phylogenies. Molecular Biology and Evolution 32(1): 268–274. https://doi.org/10.1093/molbev/msu300

O'Hara TD, Hugall AF, Thuy B, Moussalli A (2014) Phylogenomic resolution of the class Ophiuroidea unlocks a global microfossil record. Current Biology 24(16): 1874–1879. https://doi.org/10.1016/j.cub.2014.06.060

O'Hara TD, Hugall AF, Thuy B, Stohr S, Martynov AV (2017) Restructuring higher taxonomy using broad-scale phylogenomics: The living Ophiuroidea. Molecular Phylogenetics and Evolution 107: 415–430. https://doi.org/10.1016/j.ympev.2016.12.006

O'Hara TD, Rowden AA, Bax NJ (2011) A Southern Hemisphere bathyal fauna is distributed in latitudinal bands. Current Biology 21(3): 226–230. https://doi.org/10.1016/j.cub.2011.01.002

O'Hara TD, Stöhr S, Hugall AF, Thuy B, Martynov A (2018) Morphological diagnoses of higher taxa in Ophiuroidea (Echinodermata) in support of a new classification. European Journal of Taxonomy (416). https://doi.org/10.5852/ejt.2018.416

Okanishi M, Fujita T (2013) Molecular phylogeny based on increased number of species and genes revealed more robust family-level systematics of the order Euryalida (Echinodermata: Ophiuroidea). Molecular Phylogenetics and Evolution 69(3): 566–580. https://doi.org/10.1016/j.ympev.2013.07.021

Okanishi M, Kato M, Watanabe HK, Chen C, Fujita T (2020) Large populations of two new species of Ophiambix (Echinodermata, Ophiuroidea) discovered on Japanese hot vents and cold seeps. Raffles Bulletin of Zoology 68: 196–213. https://doi.org/10.26107/RBZ-2020-0017

Prokoph A, Shields GA, Veizer J (2008) Compilation and time-series analysis of a marine carbonate δ18O, δ13C, 87Sr/86Sr and δ34S database through Earth history. Earth-Science Reviews 87(3–4): 113–133. https://doi.org/10.1016/j.earscirev.2007.12.003

Rambaut A, Drummond AJ, Xie D, Baele G, Suchard MA (2018) Posterior Summarization in Bayesian Phylogenetics Using Tracer 1.7. Systematic biology 67(5): 901–904. https://doi.org/10.1093/sysbio/syy032

Ramirez-Llodra E, Brandt A, Danovaro R, De Mol B, Escobar E, German CR, Levin LA, Martinez Arbizu P, Menot L, Buhl-Mortensen P, Narayanaswamy BE, Smith CR, Tittensor DP, Tyler PA, Vanreusel A, Vecchione M (2010) Deep, diverse and definitely different: unique attributes of the world's largest ecosystem. Biogeosciences 7(9): 2851–2899. https://doi.org/10.5194/bg-7-2851-2010

Ray DC, van Buchem FSP, Baines G, Davies A, Gréselle B, Simmons MD, Robson C (2019) The magnitude and cause of short-term eustatic Cretaceous sea-level change: A synthesis. Earth-Science Reviews 197. https://doi.org/10.1016/j.earscirev.2019.102901

Revell LJ (2024) phytools 2.0: an updated R ecosystem for phylogenetic comparative methods (and other things). PeerJ 12: e16505. https://doi.org/10.7717/peerj.16505

Ronquist F, Huelsenbeck JP (2003) MrBayes 3: Bayesian phylogenetic inference under mixed models. Bioinformatics 19(12): 1572–1574. https://doi.org/10.1093/bioinformatics/btg180

Smith AB, Paterson GLJ, Lafay B (1995) Ophiuroid phylogeny and higher taxonomy: morphological, molecular and palaeontological perspectives. Zoological Journal of the Linnean Society 114(2): 213–243. https://doi.org/10.1006/zjls.1995.0024

Smith CR, De Leo FC, Bernardino AF, Sweetman AK, Arbizu PM (2008) Abyssal food limitation, ecosystem structure and climate change. Trends in Ecology and Evolution 23(9): 518–528. https://doi.org/10.1016/j.tree.2008.05.002

Stamatakis A (2014) RAxML version 8: a tool for phylogenetic analysis and post-analysis of large phylogenies. Bioinformatics 30(9): 1312–1313. https://doi.org/10.1093/bioinformatics/btu033

Stanley SM (2016) Estimates of the magnitudes of major marine mass extinctions in earth history. Proceedings of the National Academy of Sciences 113(42): E6325–E6334. https://doi.org/10.1073/pnas.1613094113

Stöhr S, O'Hara TD, Thuy B (2012) Global diversity of brittle stars (Echinodermata: Ophiuroidea). PLoS ONE 7(3): e31940. https://doi.org/10.1371/journal.pone.0031940

Stöhr S, O'Hara T, Thuy B (2025) World Ophiuroidea Database. https://www.marinespecies.org/ophiuroidea [April 30, 2025]

Stöhr S, Segonzac M (2006) Two New Genera and Species of Ophiuroid (Echinodermata) from Hydrothermal Vents in the East Pacific. Species Diversity 11(1): 7–32. https://doi.org/10.12782/specdiv.11.7

Suchard MA, Lemey P, Baele G, Ayres DL, Drummond AJ, Rambaut A (2018) Bayesian phylogenetic and phylodynamic data integration using BEAST 1.10. Virus Evolution 4(1): vey016. https://doi.org/10.1093/ve/vey016

Sun J, Zhang Y, Xu T, Zhang Y, Mu H, Zhang Y, Lan Y, Fields CJ, Hui JHL, Zhang W, Li R, Nong W, Cheung FKM, Qiu JW, Qian PY (2017) Adaptation to deep-sea chemosynthetic environments as revealed by mussel genomes. Nature ecology & evolution 1(5): 121. https://doi.org/10.1038/s41559-017-0121

Sun S, Sha Z, Wang Y (2019) Divergence history and hydrothermal vent adaptation of decapod crustaceans: A mitogenomic perspective. PLoS ONE 14(10): e0224373. https://doi.org/10.1371/journal.pone.0224373

Sun S, Xiao N, Sha Z (2023) Mitogenomes provide insights into the phylogeny and evolution of brittle stars (Echinodermata, Ophiuroidea). Zoologica Scripta 52(1): 17–30. https://doi.org/10.1111/zsc.12576

Thuy B (2013) Temporary expansion to shelf depths rather than an onshore-offshore trend: the shallow-water rise and demise of the modern deep-sea brittle star family Ophiacanthidae (Echinodermata: Ophiuroidea). European Journal of Taxonomy (48). https://doi.org/10.5852/ejt.2013.48

Vieira AR, de Sousa F, Bilro J, Viegas MB, Svanback R, Gordo LS, Paulo OS (2024) Mitochondrial genomes of the European sardine (Sardina pilchardus) reveal Pliocene diversification, extensive gene flow and pervasive purifying selection. Scientific Reports 14(1): 30977. https://doi.org/10.1038/s41598-024-82054-x

Wang K, Shen Y, Yang Y, Gan X, Liu G, Hu K, Li Y, Gao Z, Zhu L, Yan G, He L, Shan X, Yang L, Lu S, Zeng H, Pan X, Liu C, Yuan Y, Feng C, Xu W, Zhu C, Xiao W, Dong Y, Wang W, Qiu Q, He S (2019) Morphology and genome of a snailfish from the Mariana Trench provide insights into deep-sea adaptation. Nature ecology & evolution 3(5): 823–833. https://doi.org/10.1038/s41559-019-0864-8

Watling L, Guinotte J, Clark MR, Smith CR (2013) A proposed biogeography of the deep ocean floor. Progress in Oceanography 111: 91–112. https://doi.org/10.1016/j.pocean.2012.11.003

Welch AJ, Bedoya-Reina OC, Carretero-Paulet L, Miller W, Rode KD, Lindqvist C (2014) Polar bears exhibit genome-wide signatures of bioenergetic adaptation to life in the arctic environment. Genome biology and evolution 6(2): 433–450. https://doi.org/10.1093/gbe/evu025

Yang M, Gong L, Sui J, Li X (2019) The complete mitochondrial genome of Calyptogena marissinica (Heterodonta: Veneroida: Vesicomyidae): Insight into the deep-sea adaptive evolution of vesicomyids. PLoS ONE 14(9). https://doi.org/10.1371/journal.pone.0217952

Yang Z (2007) PAML 4: phylogenetic analysis by maximum likelihood. Molecular Biology and Evolution 24(8): 1586–1591. https://doi.org/10.1093/molbev/msm088

Zhang B, Zhang YH, Wang X, Zhang HX, Lin Q (2017) The mitochondrial genome of a sea anemone Bolocera sp. exhibits novel genetic structures potentially involved in adaptation to the deep-sea environment. Ecology and Evolution 7(13): 4951–4962. https://doi.org/10.1002/ece3.3067

Zhang K, Sun J, Xu T, Qiu J-W, Qian P-Y (2021) Phylogenetic Relationships and Adaptation in Deep-Sea Mussels: Insights from Mitochondrial Genomes. International Journal of Molecular Sciences 22(4). https://doi.org/10.3390/ijms22041900

Zhang L, He J, Tan P, Gong Z, Qian S, Miao Y, Zhang HY, Tu G, Chen Q, Zhong Q, Han G, He J, Wang M (2022) The genome of an apodid holothuroid (*Chiridota heheva*) provides insights into its adaptation to a deep-sea reducing environment. Communication Biology 5(1): 224. https://doi.org/10.1038/s42003-022-03176-4

Supplementary material 1

Additional tables

Authors: Weihao Xu, Jieying Na, Kexin Gao, Xinyu Gu, Yadong Zhou, Ruiyan Zhang, Jin Sun, Dongsheng Zhang

Data type: xlsx

Copyright notice: This dataset is made available under the Open Database License (http://opendatacommons.org/licenses/odbl/1.0/). The Open Database License (ODbL) is a license agreement intended to allow users to freely share, modify, and use this Dataset while maintaining this same freedom for others, provided that the original source and author(s) are credited.

Link: https://doi.org/10.3897/zse.102.163746.suppl1

Supplementary material 2

Additional information

Authors: Weihao Xu, Jieying Na, Kexin Gao, Xinyu Gu, Yadong Zhou, Ruiyan Zhang, Jin Sun, Dongsheng Zhang

Data type: docx

Copyright notice: This dataset is made available under the Open Database License (http://opendatacommons.org/licenses/odbl/1.0/). The Open Database License (ODbL) is a license agreement intended to allow users to freely share, modify, and use this Dataset while maintaining this same freedom for others, provided that the original source and author(s) are credited.

Link: https://doi.org/10.3897/zse.102.163746.suppl2